Tellus (1998), 50A, 211–218
Printed in UK – all rights reserved

TELLUS
ISSN 0280–6495

Modification of frontal circulations by surface heat flux

By HANS ØKLAND, *Department of Geophysics, University of Oslo, PO Box 1022 Blindern, 0315 Oslo, Norway*

(Manuscript received 21 April 1997; in final form 14 November 1997)

ABSTRACT

Based on Arnt Eliassen's papers on the transverse circulation at baroclinic zones, we study the influence of heat fluxes from the ocean. The paper first examines a particular weather situation over the Arctic Ocean, where a front separates very cold air over the ice cover from warmer air over the open water. The paper aims at showing that an observed increase of the wind force might be caused by the intense heating of the cold air over the water. For this purpose, we devise an analytical solution of the Eliassen equation. The fortunate location of the front in relation to the observations permits a comparison between the observed wind and the wind estimated from the equation. It is suggested that many tragic shipwrecks along the border of the ice may be explained in this way.

1. Introduction

In a remarkable paper, Eliassen (1952) demonstrated that friction and heating can drive a meridional circulation in a stable circular vortex, thereby keeping the vortex in a state of quasi-balance. He showed that such meridional perturbations on a global scale would make the westerlies narrow and cause the characteristic jet streams at tropopause level. In a later paper, using a similar technique, he extended his investigations to frontal zones in spatially varying geostrophic wind fields and showed that vertical velocity is imposed by deformation of the temperature field by the geostrophic wind (Eliassen, 1962). He has also studied the condensation at fronts and found that the released latent heat leads to a secondary circulation that tends to strengthen the front (Eliassen, 1959).

Probably, heating of the air by turbulent fluxes from the earth's surface may have a similar influence on frontal circulations, although this possibility was not specifically studied by Eliassen. It is our purpose to investigate a certain aspect of this idea. We shall connect our discussion to a spectacular intensification of the frontal wind field over the Arctic Ocean and show that the strong wind may be explained by the heat flux. Our approach will be quite general, however.

Somewhat similar ideas have been published by Moore (1991). Using a model based on theories by Hoskins and Bretherton (1972), he discusses the influence of surface heating on a frontal zone which develops as a result of a postulated hyperbolic deformation field. We shall use another approach, dictated by the fact that we have, in the critical area, a few observations which we want to reconcile.

Spatial differences in the transfer of heat is the determining factor, not the warming per se. Strong differences exist for instance along a coastline separating warm ocean water from a cold continent. As shown by Økland (1990), this may lead to characteristic changes in the wind field, notably in the component parallel to the coast. In the same paper, he suggested that the border of the arctic ice cover might have a similar effect. In fact, cases of unexpected wind behaviour have surprised meteorologists working in the area. The case we shall discuss has been brought to our attention by Kari Wilhelmsen, scientific adviser to The Norwegian Weather Service (lecture notes, 1994). An observer on a coastguard ship located south of Bear Island complained that the forecast missed an instance of very strong wind.

The synoptic scale weather condition was characterized by a strong front between North Cape on Northern Norway, and Bear Island, separating the arctic air from the warmer air mass to the south (Fig. 1). On 11 January 1993, the coast guard ship at 73°N and 17°E, reported a rapid increase of the already quite strong north-easterly gale. In fact, from 12 UT until midnight, the wind increased from 17 to 33 m/s ("hurricane force"). Only a slight wind increase was reported by the observing station on Bear Island, 100 km to the north.

The large-scale easterly wind in the area had increased somewhat during the previous day, and had veered towards northeast, in accordance with a pressure drop in the area between Bear Island and the coast of Norway. The rim of the ice cover was located between Bear Island and 73°N where the coast guard ship was heading east (Fig. 2). As seen on the map, it was oriented in an approximately sonal direction, parallel to the mean sea surface isotherms. In general, the heat transfer from the ocean is large where the wind is strong and the air-sea temperature difference is great. In the actual situation, this was probably the case since the wind blew from the ice towards the open water. The veering of the wind, mentioned above, might have started or strengthened this process. The temperature measured by the ship was $-0.3°$, while Bear Island reported $-9.4°$. The map shows a rapid increase of the sea surface temperature towards south.

A rough estimate of the sensible heat flux can be made by means of the usual gross equation

$$H = \rho C_{\mathrm{H}} c_{\mathrm{p}} V_{\mathrm{s}} (T_{\mathrm{SST}} - T_{\mathrm{air}}), \tag{1}$$

where C_{H} is the transfer coefficient, assumed here to be 0.0014 (Fujitani, 1975). Based on the observations, we have chosen V_{s} to be 25 ms^{-1} and the temperature difference to be 12 K. Then H turns out to be 0.5 kW m^{-2}. We shall make no attempt to determine the flux more accurately, nor shall we try to model it as a function of variable wind and temperature difference. Our goal will be to show that a flux density of this size may, in fact, produce a wind of the observed force.

There is, of course, also a flux of latent heat. This will be of consequence for the present study only to the extent that condensation takes place. Clouds are, in fact, observed, but theoretical considerations show that the contribution to the

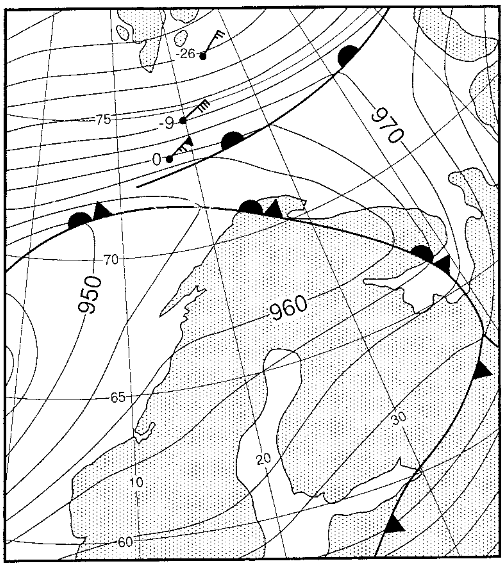

Fig. 1. Synoptic weather analyses for 12 January 1973, 00 UT, covering northern Scandinavia and parts of the surrounding seas. Three key observations of wind and temperature are plotted. They are: Hopen (76.5°N, 25°E), Bear Island (74.5°N, 19°E) and a coast guard ship (73.0°N, 17°E). Symbols and units are the standard ones.

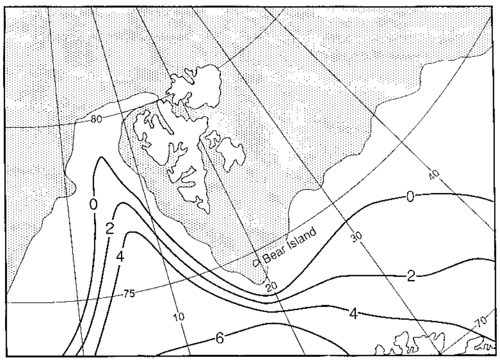

Fig. 2. Sea surface isoterms (°C) and border of sea ice for 14 January 1993.

warming is small under these conditions (Økland, 1983).

Observations are in general sparse in this area. On this specific occasion, the surface observations from the coast guard ship, and Bear Island with both surface and upper air observations, were the only reports available between Norway and Spitsbergen, a distance of more than 800 km. For these and other reasons, it would seem impossible to carry out an adequate analysis. However, the vertical structure of the atmosphere can be obtained with considerable reliability by means of the radiosonde ascents from Bear Island (Fig. 3).

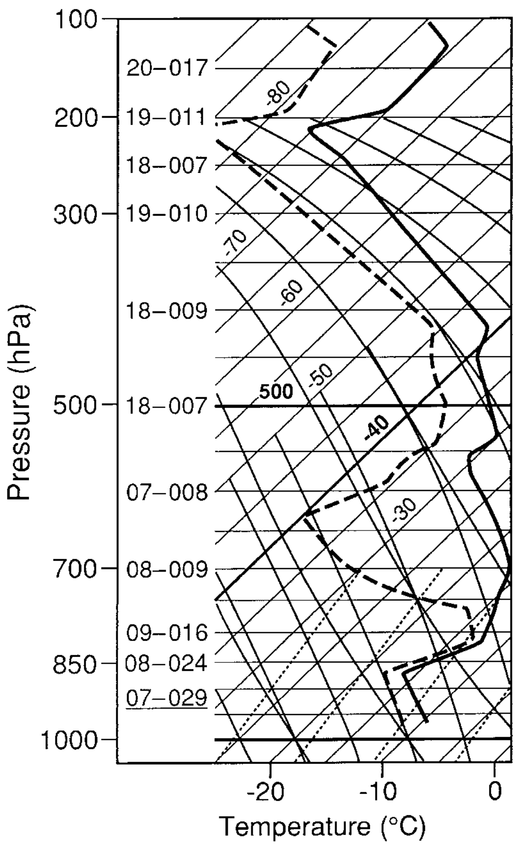

Fig. 3. Radiosonde ascent from Bear Island, 74.5°N, 19°E, on 12 January 1993, 00 UT in an oblique T, $\ln p$ diagram. Thick lines show the ordinary temperature and the dew-point temperature (dotted). Thin curves are the adiabats and the saturation mixing ratio (dotted). Wind direction (tens of degrees) and force (m/s) on the left-hand side.

In fact, the fortunate location of the radiosonde station and the observations from the near-by ship, is the reason why we venture to use this case for our purpose. We shall choose a method of investiagation which is particularly apt for this situation.

Not surprising, the upper air observations show a very strong baroclinic zone. Under such conditions, the characteristic horizontal scale is in general too small to permit the geostrophic approximation. However, the essence of the Eliassen approach is that the scale, although small in the direction across a strong baroclinic zone, may be large along the isotherms, thus permitting the assumption that the wind in this direction is in geostrophic balance with the temperature field.

In the following, we first construct the model equations (Section 2), based essentially on Eliassen's paper (1952). A formal solution is worked out in Section 3. The reader who is not specifically interested in the mathematical treatment, may skip the details. Section 4 contains a general discussion of the solution. In Section 5, we compare the theoretical results with the observations. Finally, Section 6 describes an instance of catastrophic shipwreck which we think may be explained by our theory.

2. The model

For simplicity, we apply the Boussinesq equations in a local Cartesian reference frame, with the x-axis pointing eastwards, along the front, and a parallel geostrophic wind field, U. This wind, together with the heat supplied by the ocean, is assumed to vary with y, z, and the time, t, but not with x. The same will be the case for the ageostrophic wind components, v and w, which develop in response to the heating. The momentum equation in the x direction may then be written as

$$\frac{\partial U}{\partial t} + v\frac{\partial U}{\partial y} + w\frac{\partial U}{\partial z} - fv = 0\,. \tag{2}$$

Similarly, the thrmodynamic energy equation is

$$\frac{\partial \theta}{\partial t} + v\frac{\partial \theta}{\partial y} + w\frac{\partial \theta}{\partial z} = \frac{\theta_0}{c_p T_0}\,q\,, \tag{3}$$

where θ is the departure of potential temperature from the standard value θ_0, and q the heating rate (enthalpy transferred to the mass unit per unit of time). Furthermore, we have used the thermal wind relation in the form

$$f\frac{\partial U}{\partial z}+\frac{g}{\theta_0}\frac{\partial\theta}{\partial y}=0. \tag{4}$$

Finally, from the continuity equation:

$$v=-\frac{\partial\Psi}{\partial z}$$

and

$$w=\frac{\partial\Psi}{\partial y},$$

where the stream function, Ψ, determines the vertical (transverse) circulation, identical in any yz plane.

A diagnostic equation for the transverse circulation may now be derived on the assumption that U is geostrophic anywhere and at any time. Differentiation of (4) with respect to t and inserting from (2) and (3) result in the equation:

$$A\frac{\partial^2\Psi}{\partial y^2}+2B\frac{\partial^2\Psi}{\partial y\,\partial z}+C\frac{\partial^2\Psi}{\partial z^2}=\frac{\partial E}{\partial y}, \tag{5}$$

where

$$A=\frac{g}{\theta_0}\frac{\partial\theta}{\partial z},$$

$$B=f\frac{\partial U}{\partial z}=-\frac{g}{\theta_0}\frac{\partial\theta}{\partial y},$$

$$C=f\left(f-\frac{\partial U}{\partial y}\right),$$

$$E=\frac{g}{c_p T_0}q.$$

Following Eliassen (1952), we introduce the quantity $D^2=AC-B^2$, in fact the potential vorticity, and assume that A, C and D^2 are all positive. Then (5), which is a second-order partial differential equation of elliptic type, has a single solution on the domain $z\geqslant 0$, "forced" by the right hand side, and subject to the condition that $\Psi=0$ on $z=0$ and at infinity. Since (5) is linear, the influence of heat fluxes may be added to the circulation produced by other sources. Note, however, that the transverse circulation can change A, B, C, and even E. Consequently, considered as a time-dependent problem, it is highly non-linear.

3. A formal solution based on idealized conditions

Eq. (5) may be solved numerically with A, B, C and E as known functions of y and z. In similar studies, the function values are sometimes obtained from operational data assimilation systems. We have little confidence in this procedure when the data are sparse compared to the characteristic scale of the phenomenon being investigated. Therefore, we shall use a method which depends more directly on the available observations.

It is necessary to dwell briefly on the process by which the heating takes place. We have already mentioned that the wind and the ice edge must form an angle to each other, so that there is a component of the wind blowing from the ice towards the ocean. The transfer of heat to the surface layer of the atmosphere is nearly zero over the ice, but increases rapidly as the air enters the ocean. From the surface layer, the heat spreads to higher levels by convection, thus forming a convective layer which is usually capped by an inversion, as discussed by Økland (1983) and others. The inversion serves as a barrier for the convection.

When the air mass is moderately stable, the thickness of the convective layer increases steadily downwind, rapidly in the beginning, but more slowly later on. However, if the air mass has a strong inversion at some height, as in our case, the growth of the convective layer may be halted for some distance (Fig. 3).

As shown by (5) the influence on the circulation is proportional to the horizontal derivative of the heat transfer, which clearly has its largest value close to the ice border ($y=0$). Accordingly, the larger part of the "source" is confined to a limited area in the yz-plane, narrow in the y direction and bounded in height by the thickness of the convective layer. From this, we conclude that a fairly realistic heating rate is a function of the Heaviside type, having a constant value, E_0, in an area limited by the line $z=b$, the part of the z-axis between $z=b$ and $z=0$, and the negative y-axis

(Fig. 4). Of course, b represents a characteristic height of the convective layer.

A solution of (5) may formally be written as

$$\Psi(y, z) = \int_{-\infty}^{\infty} dz_0 \int_{-\infty}^{\infty} G(y, z; y_0, z_0) \frac{\partial E}{\partial y_0} dy_0, \quad (6)$$

which defines the value of the stream function at the point (y, z) as an integral of infinitesimal "sources" of strength $(\partial E/\partial y_0)\, dy_0\, dz_0$, and where G is the Green function of the problem. It is clear from (6) that one needs to know G only at the points where the source is different from zero.

Eliassen (1952), defines a "principal" part of G as

$$\frac{1}{4\pi D_0} \ln P(y, z; y_0, z_0)$$

where

$$P(y, z; y_0, z_0) \equiv A_0(z-z_0)^2 - 2B_0(z-z_0)(y-y_0) + C_0(y-y_0)^2,$$

and the subscript zero at the coefficients signifies values in (y_0, z_0). Clearly, the contribution to the stream function Ψ from each source point is characterized by concentric elliptic streamlines. It is easily verified that this contribution satisfies the homogeneous eq. (5) but not the boundary conditions. However, if (y_0, z_0) is in the upper half plane, a "fictitious" source of the same strength, but of opposite sign, may be added at the point (y_0', z_0'), where $z_0' = -z_0$ and $y_0' = y_0 + 2B_0/C_0)z_0'$ (Fig. 4). The combined stream function is then zero on $z=0$ and at infinity. Therefore, in order to satisfy the boundary condition, a fictitious "cooling" of size $-E_0$ must be added in a domain limited by the lines $z=0$, $z=-b$, and to the left of $y=(2B_0/C_0)z$.

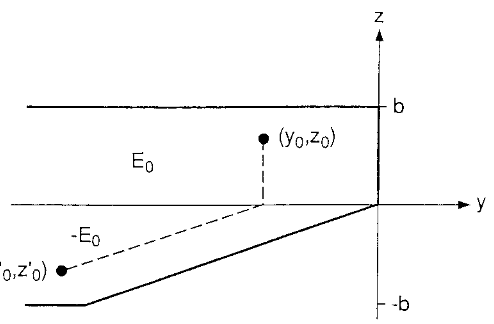

Fig. 4. Localization of the heat sources inside the heavy lines. The "real" source has a constant value, E_0, and is located above the y-axes. The "fictitious" source has the value $-E_0$, and is below the y-axes. The stream function is zero on $z=0$ if $z_0' = -z_0$ and $y_0' = y_0 + (2B/C)z_0'$. See text for further explanation.

First we consider that part ψ of Ψ, which is determined by the source in the upper half plane. Partial integration with respect to y_0 gives

$$\psi = -\int_0^b dz_0 E_0 G(y, z; 0, z_0),$$

since G is zero at infinity and the heating is limited to the strip between $z=0$ and $z=b$. From this equation, it is clear that one needs values of the coefficients only on the segment between $z=0$ and $z=b$ of the z-axis, just where the observations from Bear Island are located. Since we use only a comparatively small value of the height, b, the vertical variation may be neglected. Accordingly, we shall consider A_0, B_0, C_0 (and D_0) as constant mean values.

It will turn out to be advantageous to solve first for $\partial\psi/\partial z$. Since P is symmetric with respect to (y, z) and (y_0, z_0), one gets

$$\begin{aligned}\frac{\partial\psi}{\partial z} &= -\int_0^b dz_0 \frac{E_0}{4\pi D_0} \frac{\partial}{\partial z} \ln P(y, z; 0, z_0) \\ &= \int_0^b dz_0 \frac{E_0}{4\pi D_0} \frac{\partial}{\partial z_0} \ln P(y, z; 0, z_0) \\ &= \frac{E_0}{4\pi D_0} \ln P(y, z; 0, z_0)|_0^b. \end{aligned} \quad (7)$$

Similarly, for the fictitious source:

$$\begin{aligned}\frac{\partial\psi'}{\partial z} &= \frac{E_0}{4\pi D_0} \int_{-b}^{0} dz_0' \times \frac{\partial}{\partial z} \ln P\left(y, z; \frac{2B_0}{C_0} z_0', z_0'\right) \\ &= \frac{E_0}{4\pi D_0} \int_{-b}^{0} dz_0' \times \frac{2A_0(z-z_0') - 2B_0(y-(2B_0/C_0)z_0')}{P(y, z; (2B_0/C_0)z_0', z_0')}. \end{aligned}$$

This integral may also be solved analytically, although not so easily as in (7). The result is:

$$\frac{\partial\psi'}{\partial z}=\frac{E_0}{4\pi D_0}\frac{B_0^2-D_0^2}{B_0^2+D_0^2}\times\ln P\left(y,z;\frac{2B_0}{C_0}z_0',z_0'\right)\Bigg|_{-b}^{0}+\frac{E_0}{\pi}\frac{B_0}{B_0^2+D_0^2}\times\arctan\frac{A_0(z-z_0')+B_0(y-(2B_0/C_0)z)}{D_0(y-(2B_0/C_0)z)}\Bigg|_{-b}^{0}, \tag{8}$$

where the inverse tangent is defined to be between $-\pi/2$ and $\pi/2$. The complete solution, Ψ, may now be obtained by integrating with respect to z. There is logarithmic singularities in the points $(0, 0)$ and $(0, b)$, caused by the fact that we have introduced a discontinuity in the heating rate at $y_0=0$. Furthermore, the inverse tangent is discontinuous on $y=(2B_0/C_0)z$. The improper integral converges, however, and the stream function is continuous anywhere on $z>0$. The integral with respect to z can, in fact, be obtained by purely analytical methods. Since the result is quite complicated, it is more convenient to integrate numerically on lines $y=$constant, starting at $z=0$ where the stream function is zero. The algorithms for computing the integrand may be obtained directly from (7) and (8). An example of a stream function computed in this way is shown in Fig. 5. The heating rate, E_0, has a value corresponding to the flux density 0.5 kW m^{-2}, proposed in Section 1, and b is 1000 m, as indicated by Fig. 3. Note that $\partial\Psi/\partial z$ is the horizontal ageostrophic wind. Computed on $z=0$, it gives the horizontal leg of the transverse circulation at the surface.

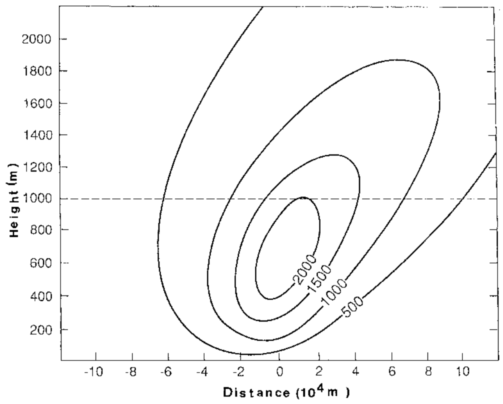

Fig. 5. Stream function in a vertical section across the front, computed by the procedure outlined in Section 3. The numerical values are: $A_0=1.4\times10^{-4}$ s^{-2}, $B_0=1.4\times10^{-6}$ s^{-2}, $C_0=2.5\times10^{-8}$ s^{-2} and $E_0=1.5\times10^{-5}$ m s^{-3}, as derived from the case study.

4. Discussion of the formal solution

Many aspects of the theory and our solution have not yet been considered here, and we shall again return to the Eliassen paper (1952). In his discussion of the forced meridional circulation of a circular vortex, he considers the properties of the principal solution in the vicinity of a single source point (x_0, y_0). The idea is that some of these properties are reflected on the large-scale structure of the transverse circulation. Below, we discuss only the case of strong baroclinicity.

If $D^2<0$, the geostrophic wind field is unstable, a fact which was discovered by Solberg (1936) and Höiland (1941), and later named symmetric instability by Hoskins (1974). It can be shown that the tilting isentropic surfaces in this case are steeper than the absolute vorticity vectors. If the structure of the wind field is such that $D^2<0$, spontaneous perturbations will lead to mixing which increases the stability (Thorpe and Emanuel, 1985).

In the stable case, when $D^2>0$, Eliassen found that the strength of the transverse adjustment circulation depends on the size of D, in such a way that a small D gives a strong circulation. In our case study, D turns out to be of about the same size as B. Accordingly, the stability of the geostrophic wind is quite strong, so that the case cannot be considered as extreme in this respect.

It is of interest for the following discussion to determine suitable scales of the transverse circulation. We want these scales to depend not only on the stream pattern imposed by the single source point, but also on the arrangement of all such points. Then, the obvious vertical scale is b, the thickness of the heated layer. Since the tilt of the transverse circulation, as noted by Eliassen (1952), is approximately equal to C_0/B_0, we propose the characteristic horizontal scale $L=B_0b/C_0$.

Additional support for this choice will appear later.

In the following we pay particular attention to $v_s = -\partial\Psi/\partial z$, the transverse ageostrophic velocity at the lower boundary of the model. The velocity may conveniently be written in the following form, where $M = D_0 b/C_0$ may be considered as an additional length scale.

$$v_s = \frac{E_0}{2\pi}\frac{D_0}{A_0 C_0}\ln\frac{y^2}{(y+L)^2+M^2} + \frac{E_0}{\pi}\frac{B_0}{A_0 C_0}\left(\arctan\frac{A_0 b + B_0 y}{D_0 y} - \arctan\frac{B_0}{D_0}\right). \tag{9}$$

Clearly, v_s vanishes when $|y| = \infty$. Furthermore, note that the first term on the right has a logarithmic singularity at $y = 0$, while the second is discontinuous. A closer inspection of (9) shows that the dominating values of v_s, roughly speaking, are confined to the interval $-L < y < 0$. On both sides of this interval, the absolute value of the velocity decreases rapidly as $|y|$ increases. This supports our choice of L as the characteristic scale.

The conclusions in the last paragraph have several implications. Most important is the fact that properties like temperature, θ, and vorticity, $-\partial U/\partial y$, tend to pack on the warmer side of $y = -L$. Accordingly, one must expect a strengthening of the front here. This frontogenetic effect of the transverse circulation has been studied by many authors. We shall not labour this point here.

The singularities in (9) are a consequence of the discontinuity we have imposed on the heating rate. With a continuous variation of E, which is physically more correct, the singularity would not exist. However, since the change from $E = 0$ over the ice to $E = E_0$ over the water, is assumed to take place over a fairly short distance, the stream function at some distance will not be much different from our solution.

The singularities are removed by integration. Therefore, in order to get a suitable characteristic value, we have computed the mean of v_s from y = 0 to $y = -L$ by integration of (9). The result may be written as

$$\overline{v_s} = \frac{E_0}{\pi}\left(\frac{D_0}{A_0 C_0}\ln\frac{B_0}{D_0} - \frac{1}{B_0}\arctan\frac{B_0}{D_0} - \frac{B_0}{A_0 C_0}\frac{\pi}{2}\right). \tag{10}$$

This equation, which determines the typical size of the transverse adjustment wind as a function of the dynamical structure of the frontal zone, is an interesting result of this study. The values of A_0, B_0, C_0 and E_0 used in the case study gives $-5.7\ \mathrm{ms}^{-1}$. One may estimate a characteristic time for the processes described, like the frontogenesis and the wind increase, as the time it takes an air parcel to move from $y = 0$ to $y = -L$, assuming that the velocity has the value computed from (10). Inserting the numerical value mentioned above, one finds that the distance L, which turns out to be 56 km, is passed in less than 3 h. This demonstrates that the characteristic scales are small indeed. However, this is, to some extent, a consequence of the discontinuity imposed on the heating rate.

We shall end this discussion with a remark on the influence of the surface friction on the ageostrophic wind, v_s. If the Ekman layer is stable, it can be described by the usual assumption that the frictional force is balanced by the Coriolis force at any level, leading to the logarithmic spiral. Thus, the Ekman layer wind is tied to v_s, assumed to be the wind "above the Ekman layer". The result usually cited is that the "true" sea surface wind is turned to the left (northern hemisphere) some 20° in relation to v_s, and reduced by a factor which depends on the Coriolis parameter and the turbulent viscosity, and often given the value 0.7 in strong winds over the sea.

5. Comment on the case study

In this section the model results will be compared to the observations. For this purpose, we estimate the expected change of the geostrophic wind by means of eq. (2), applied at the sea surface. We shall denote the geostrophic wind by $(U_s + u_s)$, where U_s is an initial value and u_s the additional wind produced by the transverse circulation. Then (2) may be written

$$\frac{\partial u_s}{\partial t} + v_s\frac{\partial u_s}{\partial y} = v_s C_0 f^{-1}, \tag{11}$$

where $C_0 = (f - \partial U_s/\partial y)f$. As earlier pointed out, the coefficients in the Eliassen equation may change by the action of the transvers circulation. However, for the relatively short time interval during which the air parcel moves from $y = 0$

to $y = -L$, this change may be neglected. Accordingly, v_s depends only on y, and eq. (11) may be integrated, giving $\Delta u_s = -C_0 f^{-1} L$. This is our estimate of the wind change brought about by the transverse circulation. The numerical value of C_0 from the case study gives $\Delta u_s = -10.0\ \mathrm{ms}^{-1}$, which is definitely of the right magnitude (Table 1). Although this result may be somewhat fortuitous considering the uncertainty in the values of the constants, we take it as an indication that our explanation of the rapid wind increase is plausible.

6. A final remark

Our interest in the problems discussed in this paper has in part been motivated by the circumstance that the area along the border of the sea ice has been considered as a dangerous place for small ships and their crew. There is usually an area of broken ice drifting in front of the solid ice cover. A strong wind may pack the drifting ice, with serious effects on the vessels which are caught in this location. Since the ice drift is to the right of the wind on the northern hemisphere, a strong wind blowing with the ice to the right might be a hazard. Many instances of shipwreck have been caused by rapid wind increase of the type studied in this paper. For instance, on 4 April 1952, 5 Norwegian boats were caught in the pack southwest of Jan Mayen, and 78 men lost their lives.

Table 1. *Wind force observed from the coast guard ship at 73°N*

Time (UT)	12	15	18	21	00	03	09
Wind (m/s)	17	25	20	25	33	33	33

7. Acknowledgements

Kari Wilhelmsen has kindly provided maps and other information. Observations from Bear Island were obtained from The Norwegian Meteorological Institute. The map of the ice edge and sea surface temperature was provided by Torgny Vinje, Norwegian Polar Institute. We have also used the Europäischer Wetterbericht, Deutscher Wetterdienst.

REFERENCES

Eliassen, A. 1952. Slow thermally and frictionally controlled meridional circulations in a circular vortex. *Astrophysica Norvegica*. **5**, 19–60.

Eliassen, A. 1959. On the formation of fronts in the atmosphere. *The Rossby memorial volume*. Rockefeller Institute & Oxford University. New York, pp. 247–260.

Eliassen, A. 1962. On the vertical circulation in frontal zones. *Geophysica Norvegica*. **24**, 147–160.

Fujitani, T., Taiichi, H. and Mitsuta, Y. 1975. Direct measurement of turbulent fluxes on R. V. Keifumaru during the AMTEX'4. *Scientific report of the 4th AMTEX Study Conference*. Tokyo. September 1975, 26–29.

Hoskins, B. J. 1974. The role of potential vorticity in symmetric stability and instability. *Quart. J. R. Met. Soc.* **100**, 480–482.

Hoskins, B. J. and Bretherton, F. P. 1972. Atmospheric frontogenesis; mathematical formulation and solution. *J. Atmos. Sci.* **29**, 11–37.

Höiland, E. 1941. *On the stability of the circular vortex*. Det Norske Videnskapsakademi i Oslo, Mat.-Naturv. Klasse, no.11.

Moore, W. G. K. 1991. Frontogenesis in the presence of surface haeting. *J. Atmos. Sci.* **48**, 63–75.

Økland, H. 1983. Modelling the height, temperature and relative humidity of a well-mixed planetary boundary layer over a water surface. *Boundary-Layer Meteorol.* **25**, 121–141.

Økland, H. 1990. The dynamics of coastal troughs and coastal fronts. *Tellus* **42A**, 444–462.

Solberg, H. 1936. *Le movement d'inertie de l'atmosphere stable et son rôle dans la theorie des cyclones*. UGGI 6th assembly, Edinburgh.

Thorpe, A. J. and Emanuel, K. A. 1985. Frontogenesis in the presence of small stability to slantwise convection. *J. Atmos. Sci.* **42**, 1809–1824.